Odd–Even Effect in the Viscoelastic Properties of Main-Chain Liquid Crystal Polymer–Low Molar Mass Nematogen Mixtures

Fu-Lung Chen and A. M. Jamieson*

Department of Macromolecular Science, Case Western Reserve University, Cleveland, Ohio 44106

*Received May 3, 1993; Revised Manuscript Received August 31, 1993**

ABSTRACT: The viscoelastic properties of dilute nematic mixtures containing 4′-(pentyloxy)-4-cyanobiphenyl (5OCB) and a main-chain liquid crystal polymer, TBP-*X*, which has a mesogenic group, 1-(4-hydroxy-4′-biphenylyl)-2-(4-hydroxyphenyl)butane, separated by flexible alkyl spacers of variable length *X*, were determined using dynamic light scattering and Freedericksz transition measurements. An odd–even variation in viscoelastic properties with spacer length of TPB-*X* was found. Specifically, TPB-2*n*/5OCB mixtures have substantially lower splay and twist decay rates and slightly higher bend decay rate than those of TPB-2*n*+1/5OCB mixtures. These differences are primarily due to changes in the associated viscosity coefficients. Comparison with existing theory leads to the conclusion that the chain configuration of TPB-*X* in 5OCB is prolate with the long axis oriented along the director ($R_\parallel/R_\perp > 1$). In addition, $R_\parallel$ of TPB-2*n* was found to be 10–20% higher than those of TPB-2*n*+1 at comparable molecular weights.

Introduction

The viscoelastic behavior of a nematic monodomain containing a liquid crystal polymer (LCP) dissolved in a low molar mass nematogen (LMMN) is a sensitive function of the LCP molecular architecture, since the chain configuration can be highly asymmetric. For example, since the shape of the LCP chain is determined by the competition between the three-dimensional entropic expansion and the tendency of the mesogenic groups to be aligned with the nematic field, the configuration of side-chain and main-chain LCP may be very different. The viscoelastic parameters which describe the splay, twist, and bend distortions of the nematic matrix can be determined via the associated Freedericksz transition characteristics under magnetic or electric fields[1,2] and by static and dynamic light scattering measurements.[3–6] In addition, the anisotropic radii of gyration, $R_\parallel$ and $R_\perp$, of the polymer chain in nematic solvent can be determined by small-angle X-ray scattering[7] or small-angle neutron scattering (SANS).[8] Finally, we note that a theoretical description of the viscosities of such mixtures has been developed by Brochard[9] which leads to expressions for the viscosity increments as a function of $R_\parallel$ and $R_\perp$.

Several investigations of the viscoelastic properties of LCP–LMMN mixtures and of the LCP chain configuration in such mixtures have been previously reported.[6–8,10–17] The major conclusions are (1) the increment of the twist viscosity, γ_1, on addition of main-chain LCP is much larger than that observed when a side-chain LCP is added;[11,14] (2) the percentage change of the various elastic constants in the presence of LCP is much smaller than that of the associated viscosities;[11,14–16] (3) the configuration of side-chain LCPs in nematic solution can be either prolate ($R_\parallel/R_\perp > 1$)[7] or oblate ($R_\parallel/R_\perp < 1$)[13,14] depending on the flexibility of the polymer chain backbone and the spacer length; (4) the configuration of main-chain LCPs in nematic solution is always prolate;[8,11,12,14] and (5) the relative decrease of the decay rate of the bend mode is small compared to those of the twist and splay modes for main-chain LCP–LMMN mixtures; however, the relative decrease of the decay rate of the bend mode is comparable to or larger than those of the twist and splay modes for side-chain LCP–LMMN mixtures.[6,17]

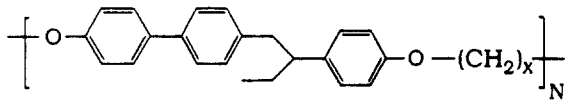

Figure 1. Chemical structure of TPB-*X*: A racemic mixture of this species was utilized in this investigation.

Of particular interest to us in this investigation is the well-known odd–even effect in the clearing temperatures of main-chain LCP which results from differences in the population of gauche and trans conformers between odd and even spacers.[18] An even–odd variation has also been observed in the miscibility of main-chain LCP with LMMN.[17,19] Since differences in the relative amount of gauche and trans conformers may lead to variations in the configurational asymmetry of the LCP in the nematic state, it is possible that there may result an odd–even oscillation in the viscoelastic behavior. In this paper we seek to discover if such an effect can be distinguished in the viscoelastic parameters of a dilute mixture of a main-chain LCP with a LMMN. So far, to our knowledge, no systematic study of such behavior has been reported. We are aware of only one investigation in which the chain anisotropy of a 10 spacer polyester measured by SANS was found to be higher than that of a 7 spacer polyester of higher molecular weight, dissolved in *p*-azoxyanisole.[8]

Experimental Section

A. Materials. The main-chain LCP, TBP-*X*,[20] consists of a mesogenic unit, 1-(4-hydroxy-4′-biphenylyl)-2-(4-hydroxyphenyl)butane, separated by flexible alkyl spacers of variable length *X*. Specimens of this main-chain LCP were supplied to us by Prof. Virgil Percec, Case Western Reserve University. The chemical structure, molecular weight, nematic isotropic transition temperature, monomer contour length, and monomer molecular weight can be found in Figure 1 and Table I. It is important to note that the polydispersities of all polymer specimens utilized in this study are comparable, $M_w/M_n \approx 2.0$, within experimental error. Thus we can safely assume that differences observed between samples are not due to variation in polydispersity. 4′-(Pentyloxy)-4-biphenylcarbonitrile (5OCB, T_{NI} = 67 °C), previously shown[19] to be a LMMN solvent for both TPB-2*n* and TPB-2*n*+1, was obtained from Aldrich Chemical Co. All materials were used as received without further purification. Polymer concentrations in all solutions were uniformly 1.00 wt %. Planar (homogeneous) monodomains were prepared using rubbed polyimide-coated conductive glass slides graciously supplied to us by Mr. Pat Dunn at Kent State University, Kent,

* Abstract published in *Advance ACS Abstracts*, October 15, 1993.

0024-9297/93/2226-6576$04.00/0

Table I. Molecular Weights, Nematic–Isotropic Transition Temperatures, Monomer Contour Lengths, and Monomer Molecular Weights of TPB-X

	TPB-7	TPB-8	TPB-9	TPB-10	TPB-11	TPB-13	TPB-14	TPB-15
M_w[a] × 10^{-4}	3.55	5.60	8.36	8.43	4.20	7.91	6.52	6.34
T_{NI},[b] °C	72	123	74	112	74	79	96	80
l_0,[c] Å	29.28	30.81	32.34	33.87	35.4	38.46	39.99	41.52
M_0[d]	414	428	442	456	470	498	512	526

[a] These data were measured by GPC using chloroform as a solvent and polystyrenes as a standard. Also note that the polydispersities of all TPB-X samples are identical, $M_w/M_n \approx 2.0$, within experimental error. [b] Data collected from second-heating DSC scans.[20] [c] l_0 is the contour length of a repeat unit. [d] M_0 is the monomer molecular weight.

OH. Homeotropic monodomains were prepared using conductive glass slides coated with lecithin (Epikuron, Lucas Meyer Inc.). Cells were filled with nematic mixtures at a temperature around 65 °C. The spacer used in the cell was 25-μm Mylar, and the cells were sealed with epoxy (Devcon). The filled sample cells were stored at 52 °C before measurement. A Carl Zeiss optical polarizing microscope equipped with a Mettler FP82HT hot stage and a Mettler FP90 central processor was used to evaluate the nematic alignment and to determine the nematic to isotropic transition temperatures, T_{NI}, of the samples. Note that the T_{NI} values reported represent the lower bound of the transition zone at a heating rate of 0.2 °C/min. The T_{NI} was measured immediately prior to any experiment. The transition zone for TPB-2n+1 solutions was very narrow (about 0.3 °C) but was wider (about 2–3 °C) for TPB-2n solutions. The T_{NI}s of mixtures were very close to that of pure 5OCB.

B. Dynamic Light Scattering. A detailed description of the methods and analytical procedures for the application of dynamic light scattering to the determination of viscoelastic parameters of nematic liquid crystals can be found elsewhere.[3-6] We performed light scattering measurements in the homodyne configuration, using a photon correlation spectrometer equipped with a 6-mW He–Ne linearly polarized laser and a BI-2030AT 264-channel digital correlator. The sample cell was positioned in a refractive index-matching bath containing 4-*tert*-butyltoluene. The sample cell temperature was controlled by a circulating bath to an accuracy of ±0.05 °C. Three VH scattering configurations which have been described in detail previously[6] were utilized in our experiments as follows:

(1) Configuration A (Splay Geometry). The director of a planar monodomain is oriented parallel to the incident polarization. The angles, θ, at which one can detect pure splay mode are (in the laboratory frame) 24.83, 26.53, and 27.51° for $\Delta T = T_{NI} - T = 5.0, 10.0$, and 15.0 °C, respectively. However, to improve the accuracy of our measurements, we also performed the scattering experiments at two additional angles displaced 1° on either side of the angle cited above, at which we still were able only to detect the pure splay mode within experimental accuracy. The decay rate, Γ_1, of the correlation function of light scattered at this geometry can be expressed by[6]

$$\Gamma_1(q) = K_{11} q_\perp^2 / \eta_{splay} \tag{1a}$$

$$q_\perp = \frac{2\pi}{\lambda_0}[(n_\parallel - n_\perp \cos\theta)^2 + n_\perp^2 \sin^2\theta]^{1/2} \tag{1b}$$

and

$$\eta_{splay} = \gamma_1 - \alpha_3^2/\eta_b \tag{1c}$$

where K_{11} is the splay elastic constant, λ_0 is the wavelength of incident light (632.8 nm), $n_\parallel$ and $n_\perp$ are the refractive indices of the extraordinary and ordinary components of nematic mixtures, θ is the scattering angle in the nematic mixture, α_3 refers to a Leslie viscosity coefficient,[21] γ_1 is the twist viscosity, and η_b is a Miesowicz viscosity.[22]

(2) Configuration B (Bend Geometry). The director of a planar monodomain is oriented perpendicular to both the incident polarization and the incident wave vector. The decay rate, Γ_2, of light scattered in this geometry is[6]

$$\Gamma_2(q) = \frac{K_{33} q_\parallel^2 + K_{22} q_\perp^2}{\eta_2} \tag{2a}$$

$$\eta_2 = \gamma_1 - \frac{\alpha_2^2 q_\parallel^2}{q_\perp^2 \eta_a + q_\parallel^2 \eta_c} \tag{2b}$$

$$q_\parallel = (2n\pi \sin\theta)/\lambda_0 \tag{2c}$$

and

$$q_\perp = 2\pi(n_\perp - n\cos\theta)/\lambda_0 \tag{2d}$$

where K_{33} and K_{22} are the bend and twist elastic constants, respectively, α_2 is a Leslie viscosity, η_a and η_c are Miesowicz viscosities, and n is the effective refractive index of the nematic mixture at the specified angle. We measured the dynamic light scattering correlation function from 16 to 43° (in the laboratory frame) because above 43° the scattering intensity was weak and not so reproducible. Note that from eqs 2a and 2b, we can determine the pure bend mode scattering if $q_\perp = 0$. At this condition, η_2 becomes the bend viscosity, η_{bend}, defined as

$$\eta_{bend} = \gamma_1 - \alpha_2^2/\eta_c \tag{3}$$

The angles (in the laboratory frame) at which we can measure the pure bend mode are 24.83, 26.53, and 27.51° for $\Delta T = T_{NI} - T = 5.0$, 10.0, and 15.0 °C, respectively.

(3) Configuration C (Twist Geometry). The director of a homeotropic monodomain is oriented perpendicular to the incident polarization and is parallel to the incident wave vector. The decay rate, Γ_2, can be expressed as[6]

$$\Gamma_2(q) = \frac{K_{33} q_\parallel^2 + K_{22} q_\perp^2}{\eta_2} \tag{4a}$$

$$\eta_2 = \gamma_1 - \frac{\alpha_2^2 q_\parallel^2}{q_\perp^2 \eta_a + q_\parallel^2 \eta_c} \tag{4b}$$

$$q_\parallel = 2\pi(n_\perp - n\cos\theta)/\lambda_0 \tag{4c}$$

and

$$q_\perp = (2n\pi \sin\theta)/\lambda_0 \tag{4d}$$

Note that we can measure the pure twist mode if $q_\parallel^2 \ll q_\perp^2$. Under this circumstance, $\eta_2 = \gamma_1$, and $\Gamma_2(q) = K_{22} q_\perp^2/\gamma_1$, from which the K_{22}/γ_1 can be determined. However, since the magnitudes of α_2 and η_c are much larger than that of η_a and since $K_{33} \sim 1.5K_{22}$, the angle at which $q_\parallel/q_\perp < 0.005$ is below 10° (in the laboratory frame). The experimental errors below such low angles are very large, due to the flare from the glass surface and the alignment uncertainty. We therefore performed measurements from 16 to 61° (in the laboratory frame).

C. Freedericksz Transition Measurement. Freedericksz transition measurements were performed to measure the splay elastic constant, K_{11}. This technique is also described in detail elsewhere.[23] Basically, this method involves monitoring the capacitance of a planar monodomain while an increasing bias voltage (V_b) is applied. The frequencies of the bias voltage and probe signal were $f_b = 50$ Hz and $f_s = 6000$ Hz, respectively. The K_{11} can be calculated via the following equation:[23]

$$V_{th}^2 = \frac{K_{11}\pi^2}{\epsilon_0 \Delta\epsilon} \tag{5a}$$

$$\Delta\epsilon = \epsilon_\parallel - \epsilon_\perp \tag{5b}$$

where V_{th} is the threshold voltage and $\Delta\epsilon$ is the dielectric anisotropy. The value of $\epsilon_\perp$ was measured at zero field and the value of $\epsilon_\parallel$ was determined by extrapolating a plot of ϵ vs $1/V_b$ to infinite voltage.[23]

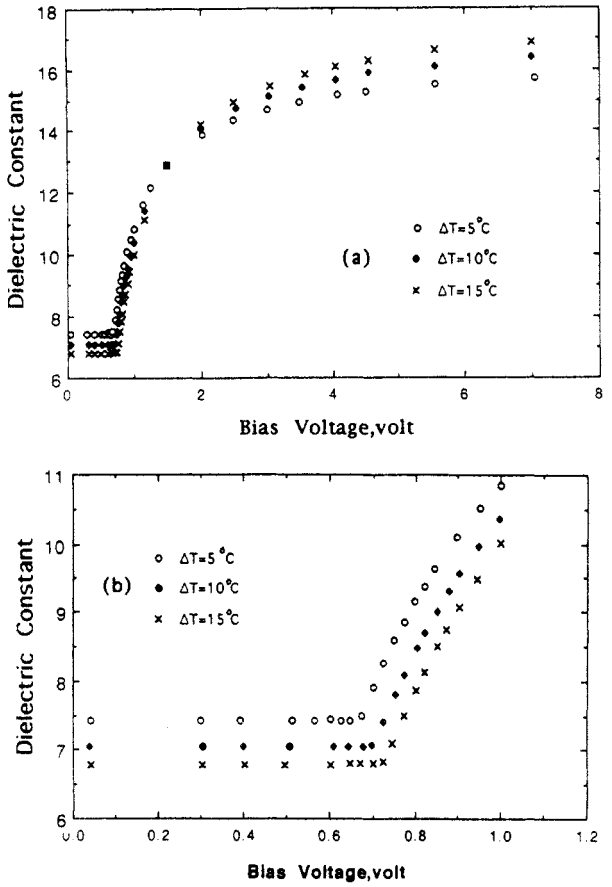

Figure 2. Results of dielectric measurements of pure 5OCB at three temperatures in the nematic state. Panel b is the enlarged transition region of panel a.

Table II. Dielectric Anisotropies and Threshold Voltages of Pure 5OCB and Mixtures at Different Temperatures

	$\Delta\epsilon \pm 1\%$			$V_{th} \pm 2\%$, V		
$T_{NI} - T$, °C	5.0	10.0	15.0	5.0	10.0	15.0
5OCB	9.04	10.32	11.17	0.669	0.704	0.728
1% TPB-7	9.08	10.44	11.34	0.670	0.695	0.712
1% TPB-8	9.30	10.49	11.40	0.696	0.723	0.745
1% TPB-9	9.58	10.61	11.42	0.675	0.700	0.719
1% TPB-10	9.51	10.79	11.62	0.692	0.714	0.737
1% TPB-11	9.52	10.64	11.49	0.675	0.694	0.710
1% TPB-13	9.48	10.57	11.39	0.679	0.709	0.729
1% TPB-14	9.63	10.78	11.66	0.686	0.717	0.737
1% TPB-15	9.49	10.76	11.55	0.674	0.698	0.719

Results and Discussion

Figure 2 shows the ϵ–V_b curves obtained for pure 5OCB in the Freedericksz transition measurements at three temperatures. The change in the dielectric constant prior to the threshold voltage is less than 0.3%, indicating that the nematic alignment of the specimen is very uniform. In Table II, the dielectric anisotropies, $\Delta\epsilon$, and the threshold voltages, V_{th}, for pure 5OCB as well as for the mixtures of TPB-X in 5OCB are listed. From this table, it is quite clear that $\Delta\epsilon$ increases slightly on addition of the polymer and the percentage increment diminishes as the ΔT ($=T_{NI} - T$) increases. Since the mixtures are very dilute (1%), it is reasonable to propose that a larger $\Delta\epsilon$ for the mixtures implies that the order parameter of TPB-X in the mixture is higher than that of pure 5OCB. This is consistent with our previous conclusion based on miscibility studies.[19] From Table II, we also deduce that there is no odd–even effect in $\Delta\epsilon$ within the experimental error. From the values of $\Delta\epsilon$ and V_{th}, the splay elastic constant, K_{11}, can be calculated using eq 5. The results are shown in Table III. In this table, K_{11} data for 5OCB from the study of Bradshaw et al.[24] are shown in parentheses. These values agree very well. Table III shows that, in general, K_{11} increases on addition of TPB-X, especially for TPB-2n. This situation is different from that encountered in mixtures containing side-chain LCP, in which the elastic constant usually is decreased.[6,16] A tendency for K_{11} to be larger has also been reported in other main-chain LCP–LMMN mixtures.[11,12,15] Another interesting feature evident in Table III is that TPB-2n mixtures always have significantly higher K_{11} than TPB-2n+1 mixtures, particularly at lower temperatures.

Table III. Splay Elastic Constants of Pure 5OCB and Mixtures

	K_{11}, 10^{-8} dyn ± 5%		
	ΔT = 5 °C	ΔT = 10 °C	ΔT = 15 °C
5OCB	36.3 (35)[a]	46.0 (47)	53.1 (56.3)
1% TPB-7	36.5	45.3	51.8
1% TPB-8	40.4	49.2	56.8
1% TPB-9	39.2	46.6	52.9
1% TPB-10	40.7	49.7	56.6
1% TPB-11	39.0	45.9	52.0
1% TPB-13	39.3	47.7	54.3
1% TPB-14	40.6	49.7	56.9
1% TPB-15	38.7	47.1	53.6

[a] The values inside the parentheses are the data of Bradshaw et al.[24]

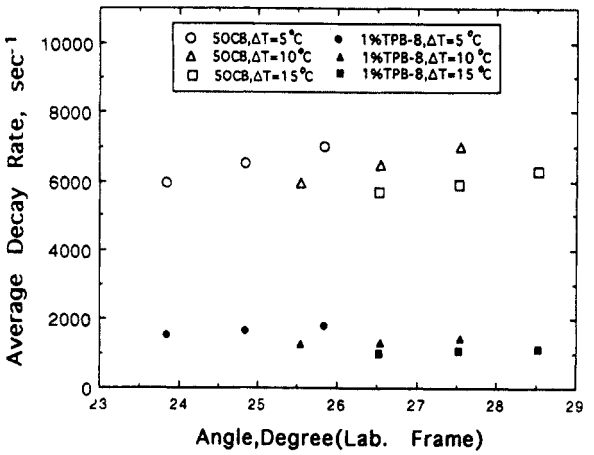

Figure 3. Average decay rates of pure 5OCB and 1% TPB-8 mixture in the splay geometry (configuration A).

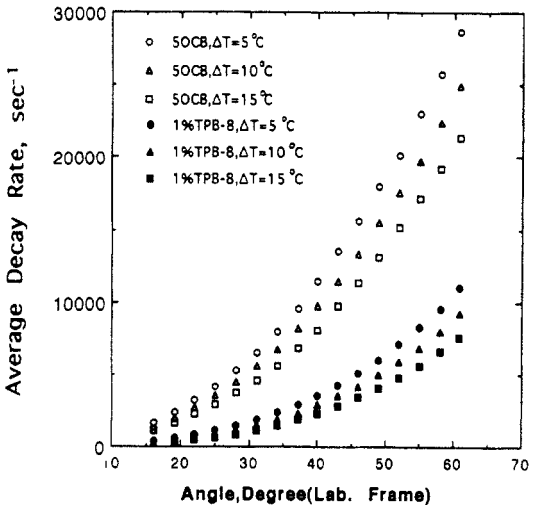

Figure 4. Average decay rates of pure 5OCB and 1% TPB-8 mixture in the twist geometry (configuration C).

The average decay rates of light scattering from pure 5OCB and from a 1% mixture of TPB-8 in 5OCB are shown in Figures 3, 4, and 5 for splay, twist, and bend geometries, respectively. As evident in Figure 5, the decay rates for the bend geometry do not change significantly

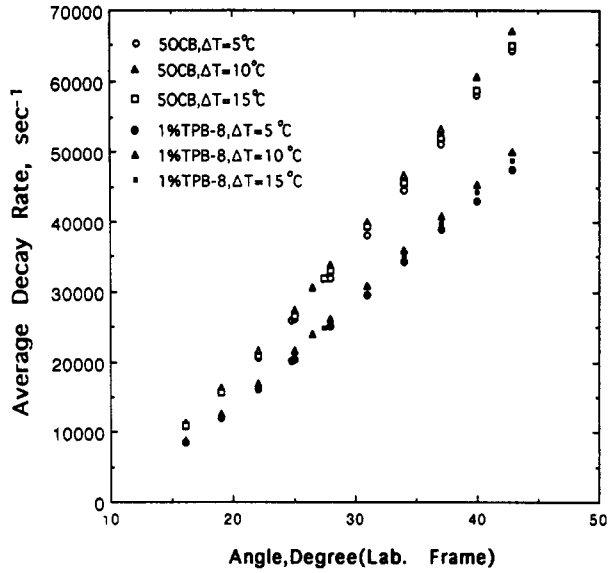

Figure 5. Average decay rates of pure 5OCB and 1% TPB-8 mixture in the bend geometry (configuration B).

with temperature, whereas from Figures 3 and 4, the decay rates for splay and twist decrease substantially with decreasing temperature. Also, the decreases in the decay rates for splay and twist on addition of TPB-*X* are much more dramatic than the corresponding change in bend. Such behavior is very consistent with that predicted by the theoretical model of Brochard[9] when the configuration of the dissolved LCP is very prolate as we will discuss in more detail later. From the fact that the splay elastic constant does not change significantly on addition of LCP (see Table III), the results in Figure 3 immediately suggest that the major factor contributing to the large decrease in the splay decay rate is an increase in the splay viscosity. From eq 1, we can directly compute the best fit value of K_{11}/η_{splay}, and since we already know K_{11}, the splay viscosity, η_{splay}, can therefore be obtained. From the definition of splay viscosity (eq 1c), if α_3 is small compared to γ_1, then

$$\eta_{splay} \approx \gamma_1 \tag{6}$$

While α_3 is known to be very small for 5CB, a published value for 5OCB is not available. To confirm that eq 6 is also valid for 5OCB, we determined the twist viscosity of 5OCB by electric field dependent dynamic light scattering measurements on a homeotropic sample cell in the twist geometry as described elsewhere[5,14] at ΔT = 15 °C. We found that the twist and splay viscosities are identical within the experimental error of 5%. This indicates that eq 6 is also applicable to our systems. Note that the thickness of the sample cells was measured before filling with the nematic mixtures at room temperature. At higher temperatures, the uncertainty in the thickness is rather high due to thermal expansion and the swelling from the refractive index-matching liquid; also, quite often the electric field dependent measurement cannot be performed successfully, probably due to the comparatively weaker anchoring strength between the glass surface and the nematogens. Because of this, we limit ourselves to reporting the splay viscosities and assume for the purpose of discussion that these are equivalent to the twist viscosities, γ_1. K_{22}/γ_1 and K_{33}/η_{bend} can be obtained by unconstrained, simultaneous curve fitting of eqs 3 and 4, with a reproducibility better than 99%. However, individual viscoelastic parameters in eq 3 or 4 with the exception of γ_1 and K_{22} must be obtained by a constrained, simultaneous curve fitting of eqs 3 and 4 in which the absolute values of α_2 are confined to a range $\gamma_1 < |\alpha_2| < 1.05\gamma_1$. This follows since α_3 is very small and $\gamma_1 = (\alpha_3 - \alpha_2)$. The reproducibility of curve fitting for η_{bend}, η_c, and α_2 is better than 95%. Several of the viscoelastic parameters obtained from curve fitting for pure 5OCB and 1% TPB-*X* mixtures are listed in Tables IV, V, and VI for ΔT = 5.0, 10.0, and 15.0 °C, respectively.

The activation energy of the twist viscosity provides a sensitive means to evaluate the coupling strength between the mesogenic group and the polymer backbone. For example, if this coupling is very weak, we can expect the activation energy of the mixture must be very close to that of the pure LMMN. Such behavior was indeed found for several mixtures containing side-chain LCPs with flexible polymer backbones.[13,25] Note that in refs 13 and 25 the activation energies quoted refer to the chain configurational relaxation times computed from the twist viscosities. We note that the activation energy of the twist viscosity is equal to that of the associated configurational relaxation time in ref 13, provided that the dielectric anisotropy is identical for pure LMMN and the mixture. The activation energy of the twist viscosity can be evaluated[26] from

$$\gamma_1/\Delta\epsilon \propto \exp(W/T) \tag{7}$$

where $\Delta\epsilon$ is the dielectric anisotropy and W is the activation energy in units of K. Since we are unable to accurately determine γ_1, for reasons mentioned above, we plot instead in Figure 6 the quantity $\eta_{splay}/\Delta\epsilon$ normalized by the value at ΔT = 5 °C. As evident in Figure 6, the corresponding activation energies are

$$W_{5OCB} = 5372 \text{ K}$$

$$W_{TPB\text{-}2n+1} = 7814 \pm 300 \text{ K}$$

and

$$W_{TPB\text{-}2n} = 8806 \pm 150 \text{ K}$$

The activation energy of 5OCB found here is almost identical to that for the twist distortion of 5CB (W = 5455 K).[13] This is not surprising because of the similarity in chemical structure, molecular size, and shape. For 1% TPB-*X* mixtures, the activation energies are much higher than that of pure 5OCB, implying that the coupling between the mesogenic group and the flexible alkyl spacer is very strong. Furthermore, the TPB-2*n* mixtures have significantly higher activation energies than those of the TPB-2*n*+1 mixtures. In other words, the TPB-2*n* are more rigid than the TPB-2*n*+1. This is consistent with the observation that the TPB-2*n* mixtures have numerically larger splay elastic constants.

To compare the effectiveness of the addition of polymer in decreasing the decay rates, we define the intrinsic inverse decay rates as

$$[\bar{\Gamma}^{-1}] = \frac{\bar{\Gamma}^{-1} - \bar{\Gamma}_0^{-1}}{C\bar{\Gamma}^{-1}} = \frac{\bar{\Gamma}_0 - \bar{\Gamma}}{C\bar{\Gamma}} \tag{8}$$

Following this, we have

$$[\bar{\Gamma}_{splay}^{-1}] = \frac{\bar{\Gamma}_{splay,0} - \bar{\Gamma}_{splay}}{C\bar{\Gamma}_{splay}} = \frac{(K_{11}/\eta_{splay})_0 - K_{11}/\eta_{splay}}{C(K_{11}/\eta_{splay})} \tag{9}$$

$$[\bar{\Gamma}_{twist}^{-1}] = \frac{\bar{\Gamma}_{twist,0} - \bar{\Gamma}_{twist}}{C\bar{\Gamma}_{twist}} = \frac{(K_{22}/\gamma_1)_0 - K_{22}/\gamma_1}{C(K_{22}/\gamma_1)} \tag{10}$$

and

$$[\bar{\Gamma}_{bend}^{-1}] = \frac{\bar{\Gamma}_{bend,0} - \bar{\Gamma}_{bend}}{C\bar{\Gamma}_{bend}} = \frac{(K_{33}/\eta_{bend})_0 - K_{33}/\eta_{bend}}{C(K_{33}/\eta_{bend})} \tag{11}$$

where C is the polymer weight concentration and subscript

Table IV. Viscoelastic Properties of Pure 5OCB and 1% TPB-*X* Mixtures at ΔT = 5.0 °C

	5OCB	TPB-7	TPB-8	TPB-9	TPB-10	TPB-11	TPB-13	TPB-14	TPB-15
$K_{11}/\eta_{splay} \pm 2\%$ (10^{-8} cm^2/s)	143.5	59.2	36.66	35.58	30.44	46.98	36.47	33.70	38.93
$K_{22}/\gamma_1 \pm 2\%$ (10^{-8} cm^2/s)	96.91	37.90	23.45	21.16	18.57	29.25	21.16	19.55	23.24
$K_{33}/\eta_{bend} \pm 2\%$ (10^{-8} cm^2/s)	679.5	516.0	528.5	508.7	520.8	494.1	518.3	530.2	515.4
$\eta_{splay} \approx \gamma_1 \pm 7\%$ (P)	0.253	0.617	1.103	1.102	1.333	0.840	1.076	1.205	0.994
$\eta_{bend} \pm 7\%$ (P)	0.0646	0.0838	0.0873	0.0906	0.0910	0.0881	0.0896	0.0876	0.0878
$\eta_c \pm 10\%$ (P)	0.372	0.757	1.263	1.291	1.483	1.006	1.272	1.355	1.188
$\alpha_2 \pm 10\%$ (P)	−0.265	−0.635	−1.133	−1.143	−1.357	−0.870	−1.120	−1.231	−1.037

Table V. Viscoelastic Properties of Pure 5OCB and 1% TPB-*X* Mixtures at ΔT = 10.0 °C

	5OCB	TPB-7	TPB-8	TPB-9	TPB-10	TPB-11	TPB-13	TPB-14	TPB-15
$K_{11}/\eta_{splay} \pm 2\%$ (10^{-8} cm^2/s)	122.8	45.74	25.65	25.78	21.76	34.62	27.17	23.76	29.45
$K_{22}/\gamma_1 \pm 2\%$ (10^{-8} cm^2/s)	80.84	28.96	17.05	15.33	13.39	22.15	15.65	13.77	17.60
$K_{33}/\eta_{bend} \pm 2\%$ (10^{-8} cm^2/s)	710.9	532.3	555.1	532.1	551.8	513.6	542.5	558.8	552.1
$\eta_{splay} \approx \gamma_1 \pm 7\%$ (P)	0.375	1.010	1.918	1.810	2.282	1.326	1.756	2.089	1.600
$\eta_{bend} \pm 7\%$ (P)	0.0815	0.1081	0.1069	0.1105	0.1111	0.1132	0.107	0.1068	0.1056
$\eta_c \pm 10\%$ (P)	0.520	1.188	2.122	2.088	2.458	1.551	2.054	2.297	1.872
$\alpha_2 \pm 10\%$ (P)	−0.391	−1.035	−1.961	−1.884	−2.310	−1.372	−1.840	−2.134	−1.672

Table VI. Viscoelastic Properties of Pure 5OCB and 1% TPB-*X* Mixtures at ΔT = 15.0 °C

	5OCB	TPB-7	TPB-8	TPB-9	TPB-10	TPB-11	TPB-13	TPB-14	TPB-15
$K_{11}/\eta_{splay} \pm 2\%$ (10^{-8} cm^2/s)	103.6	34.23	18.70	19.23	15.66	25.74	20.00	17.03	21.30
$K_{22}/\gamma_1 \pm 2\%$ (10^{-8} cm^2/s)	66.31	21.48	12.34	11.33	9.24	15.85	11.11	9.32	12.17
$K_{33}/\eta_{bend} \pm 2\%$ (10^{-8} cm^2/s)	689.5	512.0	539.7	511.4	532.7	493.6	525.3	540.2	531.4
$\eta_{splay} \approx \gamma_1 \pm 7\%$ (P)	0.512	1.515	3.037	2.755	3.613	2.035	2.715	3.340	2.519
$\eta_{bend} \pm 7\%$ (P)	0.0982	0.1322	0.1309	0.1324	0.1305	0.1368	0.1278	0.128	0.127
$\eta_c \pm 10\%$ (P)	0.686	1.715	3.286	3.089	3.822	2.322	3.098	3.578	2.833
$\alpha_2 \pm 10\%$ (P)	−0.533	−1.540	−3.090	−2.846	−3.648	−2.099	−2.831	−3.390	−2.603

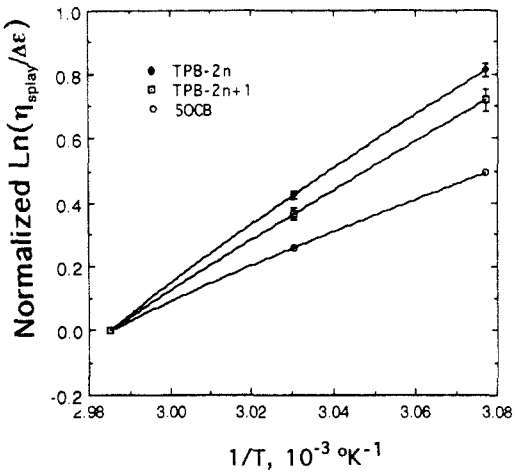

Figure 6. Temperature dependence of $\eta_{splay}/\Delta\epsilon$ for pure 5OCB and 1% TPB-*X* mixtures.

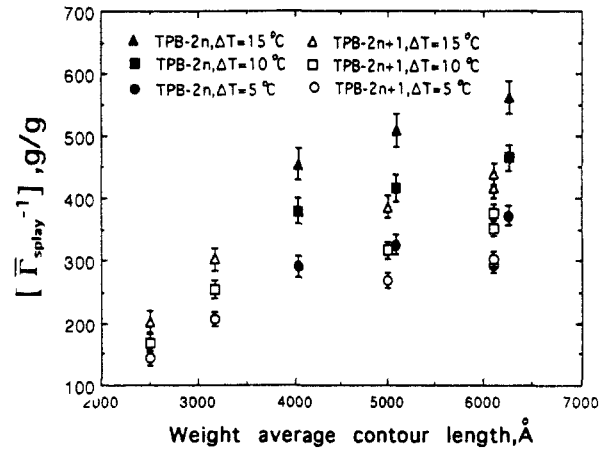

Figure 7. Intrinsic inverse splay decay rates of 1% TPB-*X* mixtures at ΔT = 5.0, 10.0, and 15.0 °C.

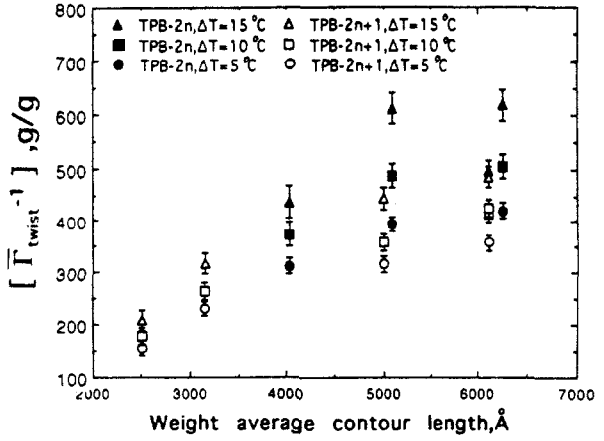

Figure 8. Intrinsic inverse twist decay rates of 1% TPB-*X* mixtures at ΔT = 5.0, 10.0, and 15.0 °C.

"0" refers to pure 5OCB. Since the change in decay rates on addition of TPB-*X* is overwhelmingly determined by the change in the associated viscosities, the $[\bar{\Gamma}^{-1}]$ are essentially numerically equivalent to an intrinsic viscosity. Because, as we expect, the molecular weight of polymer has a strong effect in the intrinsic inverse decay rates, we plot the intrinsic inverse decay rates for splay, twist, and bend modes versus the weight-average contour length, L_w, of the chain in Figures 7, 8, and 9, respectively. L_w is computed as $L_w = (M_w/M_0)l_0$ where M_0 is the monomer molecular weight and l_0 is the extended monomer contour length listed in Table I.

First, we find that the intrinsic inverse splay and twist decay rates increase strongly with a decrease of temperature and are an order of magnitude greater than the intrinsic inverse bend decay rates, which are essentially independent of temperature within the experimental error. Second, we find that there is a strong odd–even variation in the intrinsic inverse splay and twist decay rates, $[\bar{\Gamma}_{splay}^{-1}]$ and $[\bar{\Gamma}_{twist}^{-1}]$, with spacer length. More precisely, the polymers with even spacers always have higher values compared to polymers with odd spacers at the same molecular weight as seen in Figures 7 and 8. In addition, although the intrinsic inverse bend decay rates are relatively small, statistically they show an odd–even variation, the odd polymers having slightly higher values; however, these differences are within the range of absolute experimental error. To fully interpret these observations,

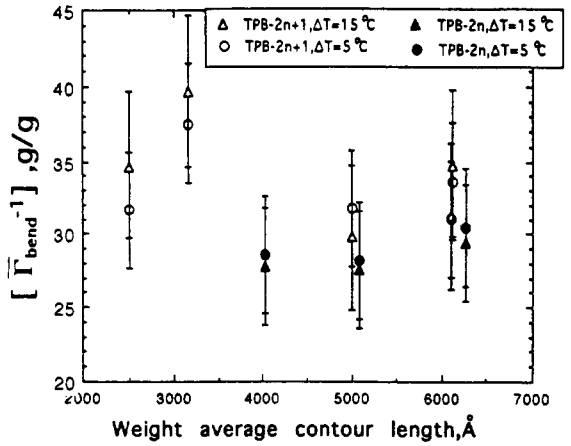

Figure 9. Intrinsic inverse bend decay rates of 1% TPB-*X* mixtures at ΔT = 5.0 and 15.0 °C.

we first present the following discussion.

From the definition of bend viscosity, η_{bend} (eq 3), and noting that $\delta\eta_{bend} = \eta_{bend} - \eta_{bend,0}$, where the second subscript "0" refers to the pure LMMN, we have

$$\delta\eta_{bend} = \delta\gamma_1 + \frac{\alpha_{2,0}^2\delta\eta_c - \eta_{c,0}(\delta\alpha_2)^2 + 2\eta_{c,0}(-\alpha_{2,0})\delta\alpha_2}{\eta_{c,0}(\delta\eta_c + \eta_{c,0})} \quad (12)$$

The theoretical model of Brochard[9] leads to the following relationships:

$$\delta\gamma_1 = \frac{cKT}{N}\tau_R\frac{(R_\perp^2 - R_\parallel^2)^2}{R_\parallel^2 R_\perp^2} \quad (13)$$

$$\delta\eta_c = \frac{cKT}{N}\tau_R\frac{R_\parallel^2}{R_\perp^2} \quad (14)$$

and

$$\delta\alpha_2 = \frac{1}{2}(\delta\gamma_2 - \delta\gamma_1) = \frac{cKT}{N}\tau_R\frac{R_\perp^2 - R_\parallel^2}{R_\perp^2} \quad (15)$$

where c is the monomer number concentration, N is the degree of polymerization, τ_R is the configurational relaxation time, and $R_\parallel$ and $R_\perp$ are the radii of gyration parallel and perpendicular to the director, respectively. For main-chain LCP, it is anticipated that the chain backbone will be oriented preferentially along the director, i.e., that the chain configuration will be prolate, with $R_\parallel > R_\perp$. From eqs 13–15, if $R_\parallel^2 \gg R_\perp^2$, then $\delta\eta_c \approx -\delta\alpha_2 \approx \delta\gamma_1$ and eq 12 becomes

$$\frac{\delta\eta_{bend}}{\delta\gamma_1} = 1 + \frac{\alpha_{2,0}^2 - \eta_{c,0}\delta\gamma_1 - 2\eta_{c,0}(-\alpha_{2,0})}{\eta_{c,0}(\delta\gamma_1 + \eta_{c,0})} \quad (16)$$

Note that if the chain configuration is spherical, i.e., $R_\parallel = R_\perp$, since $\delta\gamma_1 = 0$, $\delta\alpha_2 = 0$, eq 12 becomes

$$\delta\eta_{bend} = \frac{\alpha_{2,0}^2\delta\eta_c}{\eta_{c,0}(\delta\eta_c + \eta_{c,0})} > \delta\gamma_1 \quad (17)$$

Also, if the chain configuration is oblate, i.e., $R_\perp > R_\parallel$, from eq 12, since $\delta\alpha_2 > 0$, if $\delta\alpha_2 \le 2(-\alpha_{2,0})$, which is usually correct provided the LCP concentration is not very high, then we also have

$$\delta\eta_{bend} > \delta\gamma_1 \quad (18)$$

Therefore, the Brochard model[9] predicts that $\delta\eta_{bend} > \delta\gamma_1$ always for $R_\perp \ge R_\parallel$. In our mixtures, we find $\delta\eta_{bend} \ll \delta\eta_{splay}$ ($\approx\delta\gamma_1$) and the intrinsic splay viscosity is very large (see Figure 10), suggesting $R_\parallel^2 \gg R_\perp^2$. As a quantitative test, we compare in Table VII the experimental values

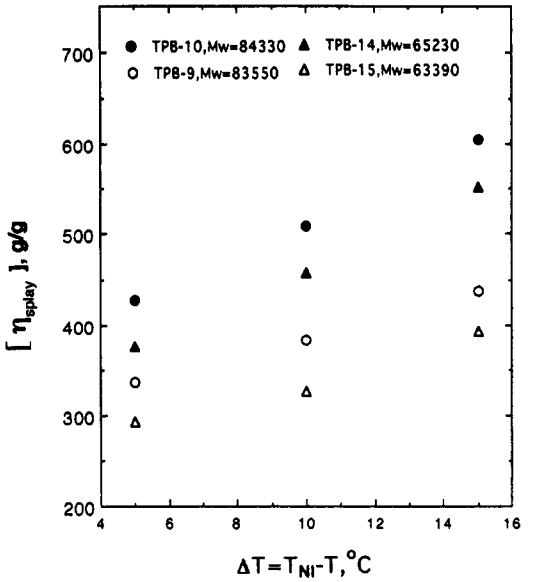

Figure 10. Temperature dependence of intrinsic splay viscosity for 1% TPB-9, 1% TPB-10, 1% TPB-14, and 1% TPB-15 mixtures.

Table VII. Comparison of Experimental (exp) and Calculated (cal) Values of $\delta\eta_{bend}/\delta\gamma_1$ of 1% TPB-*X* Mixtures Based on Equation 16

	ΔT = 5 °C		ΔT = 10 °C		ΔT = 15 °C	
	exp ± 50%	cal	exp ± 50%	cal	exp ± 50%	cal
1% TPB-7	0.053	0.042	0.042	0.028	0.034	0.020
1% TPB-8	0.027	0.025	0.017	0.016	0.013	0.011
1% TPB-9	0.031	0.025	0.020	0.016	0.015	0.012
1% TPB-10	0.024	0.021	0.015	0.013	0.010	0.009
1% TPB-11	0.040	0.032	0.033	0.022	0.026	0.015
1% TPB-13	0.030	0.026	0.018	0.017	0.013	0.012
1% TPB-14	0.024	0.023	0.015	0.014	0.011	0.010
1% TPB-15	0.031	0.028	0.020	0.018	0.014	0.013

(exp) of $\delta\eta_{bend}/\delta\gamma_1$ versus the values calculated (cal) based on eq 16. From this table, it is clear that the experimental and calculated values are numerically similar, suggesting that, indeed, $R_\parallel^2 \gg R_\perp^2$ for our main-chain LCP–LMMN mixtures.

Under this condition, eq 13 may be simplified[9] to

$$\delta\gamma_1 = \frac{c\lambda_\perp R_\parallel^2}{N} \quad (19)$$

where $\lambda_\perp$ is the frictional coefficient of the LCP in the direction perpendicular to the director. Because the chains are highly extended ($R_\parallel^2 \gg R_\perp^2$), it is reasonable to assume the hydrodynamic behavior is free draining, in which case we may write[9]

$$\lambda_\perp = Nl_0z_\perp \quad (20)$$

where $z_\perp$ is the friction coefficient per unit length between the polymer chain and the LMMN solvent and l_0 is the contour length of the monomer. Therefore eq 19 can be further expressed as

$$\delta\gamma_1/(cl_0) = z_\perp R_\parallel^2 \quad (21)$$

If we contrast the behavior of polymers with proximate spacer lengths, for example TPB-9 versus TPB-10 or TPB-14 versus TPB-15, the $z_\perp$ in eq 21 can be reasonably assumed to be identical for each pair. In this case, we can compare the chain extensions, $R_\parallel$, for the polymer pair. In Table VIII we show results of such analysis for TPB-9/TPB-10 and TPB-14/TPB-15 polymer pairs which have similar molecular weights. From this table, we find, as expected, that the even-spacer polymers have larger

Table VIII. Comparison of $R_\parallel$ for TPB-9/TPB-10 and TPB-14/TPB-15 at Different Temperatures

$T_{NI} - T$, °C	$R_{\parallel,TPB-10}/R_{\parallel,TPB-9}$	$R_{\parallel,TPB-14}/R_{\parallel,TPB-15}$
5.0	1.12	1.14
10.0	1.14	1.19
15.0	1.17	1.19

$R_\parallel$—i.e., the chains are more extended—and that the difference in the degree of extension between even- and odd-spacer polymer increases as the temperature decreases, i.e., as the order parameter increases. Yoon et al.[27] have estimated the chain sequence extension of some main-chain LCPs in the bulk state based on conformational energy calculations. For $[-OpC_6H_4COOpC_6H_4O(CH_2)_n^-]_x$, their analysis indicated a most probable chain extension when $n = 10$ of 23 Å and when $n = 9$ of 19 Å, leading to an extension ratio of 1.2. The ratios listed in Table VIII are of comparable magnitude to this. This is almost certainly fortuitous. However, we note that the value of $R_\parallel$ will be determined principally by the probability of hairpin formation, which will increase with gauche content of the spacer. The number of hairpins should be larger for odd versus even polymers, leading to a smaller $R_\parallel$.

The above observations indicate that TPB-2n has a higher rigidity than TPB-2n+1 because the TPB-2n chain is more extended. Likewise, the larger intrinsic inverse splay and twist decay rates of TPB-2n also reflect the more extended chain configuration of TPB-2n because the splay and twist deformations involve chain rotation. Thus, the more extended the chain, the more difficult is the deformation. The rationale for TPB-2n mixtures having smaller intrinsic inverse bend decay rates (i.e., higher bend decay rates) could be interpreted as due to TPB-2n having a higher extension, i.e., a smaller cross-sectional area since the bend viscosity involves a sliding displacement parallel to the backbone.[28]

Finally, we draw attention to the temperature dependence of the intrinsic splay viscosity. One expects there may be two contributions to this in LCP–LMMN mixtures, namely, the excluded volume and the strength of the nematic field (order parameter effect). The former will cause the intrinsic viscosity to decrease with a decrease of temperature because of a weaker interaction between polymer and LMMN at lower temperatures. In contrast, the latter will cause an increase in the intrinsic viscosity at lower temperatures because the order parameter is higher. In Figure 10, we plot the intrinsic splay viscosity as a function of the temperature increment $\Delta T = T_{NI} - T$. From Figure 10, it is very clear that the intrinsic splay viscosity increases strongly with decrease of temperature, which immediately implies that the order parameter overrides the excluded volume effect in our systems. In addition, it is pertinent to note that the molecular weight values quoted here and in Table I were determined by GPC. Thus Figure 10 demonstrates unequivocally that for TPB-X polymers which have essentially the same hydrodynamic volume in the isotropic state, $[\eta_{splay}]$ is substantially larger in the nematic state for $X = 2n$ than for $X = 2n + 1$ or $2n - 1$.

Conclusions

We have observed an odd–even variation with spacer length of main-chain LCP in the viscoelastic properties of dilute LCP–LMMN mixtures. The pure splay and twist decay rates decrease more strikingly than the pure bend decay rate on addition of TPB-X. The odd–even variation is manifested by TPB-2n mixture having higher splay elastic constant, higher rigidity, higher splay viscosity, and higher pure bend decay rate than the mixture containing TPB-2n+1 with the same molecular weight. The results are consistent with the idea that the chain of TPB-2n is more extended. We also showed that the presence of a highly prolate configuration, i.e., $R_\parallel^2 \gg R_\perp^2$, is supported by the fact that the experimental values of $\delta\eta_{bend}/\delta\gamma_1$ agree with the values calculated based on the Brochard model. Invoking the Brochard theory and a free-draining condition, $R_\parallel$ of TPB-2n in solution was found to be 10–20% higher than that of TPB-2n+1 of similar molecular weight. Finally, from the temperature dependence of the intrinsic splay viscosity, we concluded that the nematic field effect is dominant over the excluded volume effect in the determination of hydrodynamic properties of our LCP–LMMN mixtures.

Acknowledgment. We would like to thank Prof. Virgil Percec of Case Western Reserve University for kindly supplying the main-chain LCP. Also, we thank Mr. Pat Dunn at Kent State University for providing the polyimide-coated glass slide. Finally, financial support from NSF Materials Research Grant DMR 01845 is gratefully acknowledged.

References and Notes

(1) Brochard, F.; Pieranski, P.; Guyon, E. *J. Phys. (Fr.)* **1972**, *33*, 681; **1973**, *34*, 35.
(2) Brochard, F.; Pieranski, P.; Guyon, E. *Phys. Rev. Lett.* **1972**, *28*, 1681.
(3) Orsay Liquid Crystal Group *J. Chem. Phys.* **1969**, *51*, 816.
(4) Orsay Liquid Crystal Group *Phys. Rev. Lett.* **1969**, *22*, 1361.
(5) Sefton, M. S.; Bowdler, A. R.; Coles, H. J. *Mol. Cryst. Liq. Cryst.* **1985**, *129*, 1.
(6) Gu, D.; Jamieson, A. M.; Rosenblatt, C.; Tomazos, D.; Lee, M.; Percec, V. *Macromolecules* **1991**, *24*, 2385.
(7) Mattoussi, H.; Ober, R. *Macromolecules* **1990**, *23*, 1809.
(8) D'Allest, J. F.; Sixou, P.; Blumstein, A.; Blumstein, R. B.; Teixeira, J.; Noriez, L. *Mol. Cryst. Liq. Cryst.* **1988**, *155*, 581.
(9) Brochard, F. *J. Polym. Sci., Polym. Phys. Ed.* **1979**, *17*, 1367.
(10) Weill, C.; Casagrande, C.; Veyssie, M. *J. Phys. (Fr.)* **1986**, *47*, 887.
(11) Mattoussi, H.; Veyssie, M. *J. Phys. (Fr.)* **1989**, *50*, 99.
(12) Pashkovsky, E. E.; Litvina, T. G. *J. Phys. (Fr.) II* **1992**, *2*, 521.
(13) Pashkovsky, E. E.; Litvina, T. G.; Kostromin, S. G.; Shibaev, V. P. *J. Phys. (Fr.) II* **1992**, *2*, 1577.
(14) Gu, D.-F.; Jamieson, A. M.; Lee, M.-S.; Kawasumi, M.; Percec, V. *Liq. Cryst.* **1992**, *12*, 961.
(15) Gilli, J. M.; Sixou, P.; Blumstein, A. *J. Polym. Sci., Polym. Lett. Ed.* **1985**, *23*, 379.
(16) Coles, H. J.; Sefton, M. S. *Mol. Cryst. Liq. Cryst. Let.* **1985**, *1*, 159.
(17) Gu, D.; Jamieson, A. M.; Kawasumi, M.; Lee, M.; Percec, V. *Macromolecules* **1992**, *25*, 2152.
(18) Marcelja, S. *J. Chem. Phys.* **1974**, *60*, 3599.
(19) Chen, F.-L.; Jamieson, A. M. *Liq. Cryst.* **1993**, *15*, 171.
(20) Percec, V.; Kawasumi, M. *Macromolecules* **1991**, *24*, 6318.
(21) Leslie, F. M. Q. *J. Mech. Appl. Math.* **1966**, *19*, 357.
(22) Miesowicz, M. *Bull. Int. Acad. Pol. Sci. Lett., Ser. A* **1936**, *28*, 228.
(23) Meyerhofer, D. *J. Appl. Phys.* **1975**, *46*, 5084.
(24) Bradshaw, M. J.; Raynes, E. P.; Bunning, J. D.; Faber, T. E. *J. Phys. (Fr.)* **1985**, *46*, 1513.
(25) Mattoussi, H.; Veyssie, M.; Casagrande, C.; Guedeau, M. A. *Mol. Cryst. Liq. Cryst.* **1987**, *144*, 211.
(26) Prost, J.; Sigaud, G.; Regaya, B. *J. Phys. Lett. (Fr.)* **1976**, *37*, L341.
(27) Yoon, D. Y.; Bruckner, S. *Macromolecules* **1985**, *18*, 651.
(28) Taratuta, V.; Hurd, A. J.; Meyer, R. B. *Phys. Rev. Lett.* **1985**, *55*, 246.